Vol. 10(35), Jan. 2020, PP. 4493-4501

Contents list available at IJMEC

International Journal of Mechatronics, Electrical and Computer Technology (IJMEC)

Journal Homepage: www.aeuso.org

PISSN: 2411-6173 - EISSN: 2305-0543

Acoustical Direction Finding using a Bayesian Regularized Multilayer Perceptron Artificial Neural Networks on a Tri-Axial Velocity Sensor

Chibuzo Joseph Nnonyelu[1] and Zakayo Ndiku Morris[2]

[1]*Dept. of Electrical Engineering, University of Nigeria, Nsukka, Nigeria*

[2]*Dept. of Electronic and Info. Engineering, Hong Kong Polytechnic University, Hong Kong*

Phone Number: *+234-9086235671*

****Corresponding Author's E-mail:*** chibuzo.nnonyelu@unn.edu.ng

Abstract

A two-dimensional direction-of-arrival estimation scheme based on Bayesian-regularized (BR) Multilayer Perceptron (MLP) artificial neural network (ANN) is developed around a unit acoustic vector sensor (AVS). The AVS basically consists of three collocated and orthogonally oriented velocity sensors, hence, senses acoustic waves in the three Cartesian directions while offering portability in size and simplicity in its array manifold. It is shown that the Bayesian regularized Multilayered Perceptron neural network performs well in terms of estimation's root-mean-square error even when tested with data of different signal-to-noise ratio (SNR) after training. This is useful as it accounts for unexpected changes of received data SNR during field operation. The proposed system is ideal for applications in mobile systems such as robots for search-and-rescue operations or soldiers in the battle field to estimate the source of a sniper fire.

Keywords: *Acoustic direction finding, acoustic position measurement, acoustic signal processing, acoustic vector sensor, artificial neural network, Bayesian regularization, multilayered perceptron.*

1. Introduction

Direction finding in acoustics involves the estimation direction(s) from which sound wave(s) arrive at an acoustic sensor array. This area of research has attracted interest from companies, institutions and governments due to its applications in consumer products (e.g. smarts speakers such as Google Home and Amazon Echo [1]), naval warfare and navigation (e.g. SONAR), and gunfire locator [2]. Acoustic direction finding can find application is search-and-rescue operation. After natural disaster, the site can be inaccessible by humans hence a robot is ideal for navigating through the area and locating victims by either image processing technology, acoustic signal processing technology, or a combination of both. A search-and-rescue robot's auditory system should have (1) sound source localization technology to estimate the direction from which the sound emanates, (2) sound source separation technology to isolate a sound source from many other sources, and (3) automatic speech recognition technology to extract human voice from background noise [3]. This investigation is focused on sound source localization and assumes there is another technology in place for sound separation and speech recognition. In robotics, navigation using sound (SONAR) has also been applied. Autonomous robots utilize acoustic direction finding for sound source localization and for obstacle detection [4], [5]. After a natural or artificial disaster, these search and rescue robots equipped with microphones, among other sensors, can be used to track and rescue victims in disaster areas by tracking the direction from which victims' voices emanate from and also to detect obstacle on its way to the victim [3], [4]. One of such robots was designed and

Article History:
Received Date: Apr. 14, 2019
Accepted Date: Jun. 11, 2019
Available Online: Jan. 01, 2020

built by Huang et. al [5] in which 3 omnidirectional microphones arrange in equilateral triangular form on the horizontal plane.

To ensure the agility of such robots is not compromised, it becomes ideal to fit a sensor that relatively smaller thereby reducing the overall size of the robot. The acoustic vector sensor consists of three orthogonally oriented and spatially collocated particle velocity sensors [6]. This spatial collocation eliminates the phase angle in its array manifold hence making its array manifold independent of the source frequency. This reduces the complexity of signal processing technique which would have required an extra processing to decouple the frequency information from the array manifold and at the same time is physically compact. Microflown produces a commercially available AVS which was implemented using MEMS (Micro-Electro-Mechanical Systems) technology [7].

The near-field and far-field array manifold of the acoustic vector sensor have been proposed and studied in [8],[9] and the case of non-perpendicular acoustic vector sensor has been studied in [10]. Three-dimensional source localization algorithm using the AVS based on eigen-decomposition is proposed in [11]. But these methods assume a certain type of noise distribution and performs poorly at low signal-to-noise ratio.

Machine learning has been applied to acoustic direction finding since more than two decades [12]-[34], [36]-[42]. In these literatures, [13]-[21], [24]-[26], [28], [31], [33]-[37] used a uniform linear array; [22] used the L-shaped array; [27], [32], [39] used the uniform circular array; and [23],[40] used the uniform rectangular array, all of various number of isotropic sensors. The array manifolds of phased arrays are complex-valued, hence the input nodes of any neural network account for the real and imaginary values which thereby increases the dimension of the input node.

The Multi-Layered Perceptron (MLP) artificial neural network of various number of hidden layers, number of input nodes, and number of output nodes were used in [12]-[22]. In the MLP literatures, [13], [14], [21] used the backpropagation training algorithm while [15]-[20], [22] used the Levenberg-Marquardt training algorithm hence not considering the noisiness of the training data. Also, none of these MLP literatures proposed a 2-dimensional (polar angle and azimuth angle) direction of arrival (DOA) estimation algorithm.

In this paper, a 2-dimensional DOA estimation BR-MLP-ANN direction finding system on a single acoustic vector sensor is proposed. This has the advantage of physical portability due to the geometry of the AVS, reduced dimension of the input layer due to the real-valued array manifold, and good performance with noisy data of any noise statistics since the BR method considers the statistics of the network weight in choosing the best model during training.

In the rest of this paper, the array manifold of the acoustic vector sensor and the statistical model of the measured data is developed in Section 2. Section 3 describes the structure and parameters of the proposed network and algorithm. Section 4 discusses the result of the training and testing of the network. Finally, Section 0 concludes the paper.

2. Data Models

This section introduces the array manifold of the acoustic vector sensor in Section 2-2.1. The statistical model of the data gathered by this AVS is discussed in Section 2-2.2.

2.1. The Tri-axial Velocity Sensor Array Manifold

For a point source, (in the far field or the near field), emitting a signal *through a quiescent fluid medium*}, reaching a tri-axial velocity-sensor *not* near any reflecting boundary, the Nehorai-Paldi model [6], [8] gives an array manifold of

$$\mathbf{a}(\theta,\phi) = \begin{bmatrix} \cos(\phi)\sin(\theta) \\ \sin(\phi)\sin(\theta) \\ \cos(\theta) \end{bmatrix} \qquad (1)$$

where $\theta \in [0, \pi/2]$ refers to the incident source's polar angle (measured from the positive z-axis), and $\phi \in (-\pi, \pi]$ symbolizes the azimuth angle (measured from the positive x-axis).

2.2. The Statistical Model of the Measured Data

At the discrete-time instant p, the tri-axial velocity-sensor collects this 3×1 data:

$$\mathbf{z}(p) := \mathbf{a}(\theta, \phi)s(p) + \mathbf{n}(p), \tag{2}$$

where $\{s(p), \forall p\}$ denotes the incident signal, $\{\mathbf{n}(p), \forall p\}$ refers to the additive noise, and $p = 1, 2, \cdots, P$ is the discrete time variable with P being the total number of time sample of the received data.

The incident signal is a pure tone $s(p) = \mathrm{R}\{e^{j2\pi f_o p + j\varphi}\}$, where $f_o \in [0,1]$ symbolizes the tone's digital frequency and $\varphi \in [0, 2\pi)$ denotes the initial phase. A pure tone has a bandwidth of zero, of course. The human voice spans a range of frequency. However, it is assumed that a voice detection technology has been used to detect the presence of human voice and isolate it from other sound sources. This isolated voice is then decomposed into various frequency bins by Discrete Fourier Transform and the highest frequency-bin selected as the pure tone signal for the proposed algorithm.

The additive noise's temporal statistics may also be modeled as

(a) a random noise sequence, that is uncorrelated over time, but Gaussian distributed with a zero mean and a σ_n^2 variance for all p,

(b) a random noise sequence, that is correlated over time, and/or non-Gaussian distributed, and/or with a non-zero and time-varying mean, and/or with a time-varying $\sigma_n^2(p)$ variance,

among other possibilities. Moreover, $\{\mathbf{n}(p), \forall p\}$ has a spatial statistic that need to be modeled. Possibilities include:

Spatially white noise (spatially incoherent) with a zero mean and a spatio-temporal correlation matrix of $\mathbf{R}_n(\tau) := \mathrm{E}[\mathbf{n}(p)\mathbf{n}^H(p+\tau)] = \sigma_n^2(\tau)\mathbf{I}_3$, where the superscript ^{H} denotes the Hermitian operator, $\sigma_n^2(\tau)$ refers to the noise's temporal autocorrelation, and I_3 symbolizes a 3×3 identity matrix. A degenerate case of (a) is spatio-temporally white noise of power σ_n^2. Then, $\mathbf{R}_n(\tau) = \sigma_n^2\delta(\tau)\mathbf{I}_3$.

3. Training set and algorithm

In this section, the training data is developed and algorithm for the network training is introduced.

3.1. Reduction of the Data Dimensionality

The received data $\mathbf{z}(\theta, \phi, p)$ in (2) has three degrees-of-freedom and random since it is corrupted by a random additive noise. Eigen-based parameter estimation algorithm estimates the incident source's steering vector as an intermediate step. This estimation is correct to only within an unknown complex-valued scalar of c [43]. That is, available to the estimation's subsequent algorithmic steps would be $\hat{\mathbf{a}} \approx c\,\mathbf{a}(\theta, \phi)$, the principal eigen-vector of the covariance matrix of the received data. This approximation would asymptotically become equality as the number of time-samples P increases toward infinity or as the noise power drops toward zero, and similarly for subsequent approximations.
The norm of the array manifold of the acoustic vector sensor $\|\mathbf{a}(\theta, \phi)\| = 1 \implies \|\hat{\mathbf{a}}\| = \mathrm{c}$. The proposed system will exploit the unity norm of the array manifold of the acoustic vector sensor in eliminating the unknown c from the estimated steering vector by dividing it by its Euclidean norm. Hence, we define for all the time samples,

$$\mathbf{x} = \hat{\mathbf{a}}/\|\hat{\mathbf{a}}\| \tag{3}$$

for each direction (θ, ϕ). Thus, reducing the degree-of-freedom of the input data from three (θ, ϕ, p) to two (θ, ϕ).

3.2. Input Data and Input Nodes

The training input data matrix, $\mathbf{X}$ is form as

$$\mathbf{X} \coloneqq [\mathbf{x}(1), \mathbf{x}(2), \cdots, \mathbf{x}(M)], \qquad \in \mathcal{R}^{3\times\mathcal{M}} \tag{4}$$

where M is the total number of training samples.

The system proposed in this paper would require a network of 3 input nodes, which reduces the computational resources required for training the network. This is a significant improvement when compared to the higher number of input nodes greater than 6 as used in [13]-[34], [36]-[42].

3.3. Hidden Layer

Single-hidden-layer MLP neural network is considered in this paper. The multi-layered perceptron network can be used for any sort of input-output mapping. An MLP network with one hidden layer and enough neurons in the hidden layer, can fit any finite input-output mapping problem [44]. For the function approximation task, the tan-sigmoid activation function has been shown to offer a faster convergence rate compared to other similar activation function. This is because of its slow saturation rate.

To determine the best number of hidden neurons for the network, the network will be trained with 10, 20, 30, 40, 50, and 60 number of hidden neurons (other parameters unchanged), and the best selected.

3.4. Output Data and Nodes

The network has two output nodes (polar angle θ and azimuth angle ϕ), thus for the mth training sample, the output of the network $y(m) = [\theta_m, \phi_m]^T$. The collection of the training sample target outputs

$$\mathbf{Y} \coloneqq [\mathbf{y}(1), \mathbf{y}(2), \cdots, \mathbf{y}(M)], \in \mathcal{R}^{2\times\mathcal{M}} \tag{5}$$

where all other variables are as previously defined.

The output of the network will be a weighted linear combination of the neurons in the hidden layer. Therefore, the two output neurons have a linear activation function.

3.5. Training Algorithm

Back propagation by gradient descent [45] and other gradient-only-based learning algorithms that minimizes the mean-square error or sum-of-square error cost functions would perform poorly due to the noisy training data. They are also prone to overfitting and require extra data for validation during training. These algorithms do not consider the probability distribution of training data and the posterior probability of the network's weights.

The network is trained with data $D = \{\mathbf{x}(m), \mathbf{y}(m)\}$ by iteratively adjusting $\mathbf{w}$ to minimize the sum of square error function

$$E_D(\mathbf{w}) = \frac{1}{2}\sum_{m}\sum_{i}\left(y_i(m) - f_i(\mathbf{x}(m); \mathbf{w})\right)^2, \tag{6}$$

where $y_i(m)$ denotes the target for the ith output node for the mth training point, $\mathbf{x}(m)$ is the input vector of the mth training point, $\mathbf{w}$ is the network's weight vector, and $f_i(\mathbf{x}(m); \mathbf{w})$ denotes the activation function of the ith neuron in the output layer. The cost function of the network is regularized as

$$M(\mathbf{w}) = \beta E_D + \alpha E_W \tag{7}$$

where $E_W = \frac{1}{2}\sum_i w_i^2$. This additional term decreases the tendency of overfitting the noise in the training data by favoring small values of the network weights.
The cost function can be interpreted as minus log likelihood for a noise model

$$P(D|\mathbf{w}, \beta, \mathcal{H}) = \frac{1}{Z_D(\beta)} \exp(-\beta E_D), \tag{8}$$

and likewise, the regularization term can be interpreted as a minus log prior probability distribution over the parameters

$$P(\mathbf{w}|\alpha, \mathcal{H}) = \frac{1}{Z_w(\alpha)} \exp(-\alpha E_W) \tag{9}$$

In the above expressions, the distributions of the data and the prior are Gaussian with β defining a noise level $\sigma_v^2 = \beta^{-1}$ for (8), and $\sigma_W^2 = \alpha^{-1}$ is the variance of the distribution in (9).

Therefore, the cost function (7) corresponds to the inference of $\mathbf{w}$ given data

$$\begin{aligned} \mathrm{P}(\mathbf{w}|D, \alpha, \beta, \mathcal{H}) &= \frac{P(D|\mathbf{w}, \beta, \mathcal{H}) P(\mathbf{w}|\alpha, \mathcal{H})}{P(D|\alpha, \beta, \mathcal{H})}, \\ &= \frac{1}{Z_m} \exp\big(-M(\mathbf{w})\big) \end{aligned} \tag{10}$$

where $\mathcal{H}$ denotes the ith model. The backpropagation methods with gradient descent is used to estimate the network weight $\mathbf{w}_{\mathrm{mp}}$ that minimizes eq. (10). The log-posterior is Taylor-expanded with $\Delta\mathbf{w} = \mathbf{w} - \mathbf{w}_{\mathrm{mp}}$ as

$$P(w|D, \mathcal{H}_i) \approx P\left(w_{\mathrm{mp}}\middle|D, \mathcal{H}_i\right) \exp\left(-\frac{1}{2} \Delta\mathbf{w}^{\mathrm{T}} \mathbf{A}\, \Delta\mathbf{w}\right) \tag{11}$$

where $\mathbf{A} = -\nabla\nabla \log P\,(w|D, \mathcal{H}_i)|_{\mathbf{w}_{\mathrm{mp}}}$ is the error bar obtained as the Hessian of the log-posterior at $\mathbf{w}_{\mathrm{mp}}$. Thus, the posterior can be approximated as a Gaussian with covariance matrix $\mathbf{A}^{-1}$.
The next level of inference determines the most plausible model given the data. Therefore, we define the posterior probability of each model as

$$P(\mathcal{H}_i|D) \propto P(D|\mathcal{H}_i) P(\mathcal{H}_i) \tag{12}$$

For more details on the development of the Bayesian Regularization please refer to [46], [47]. The Bayesian regularization algorithm is implemented in MATLAB neural network toolbox. This toolbox is used for training and testing of the proposed method.

4. Simulation Results

Different training scenarios were carried out to determine the optimum number of hidden neurons H and learning rate μ. The range of the polar angle is limited to $\theta \in [90°, 120°]$. This is because for an autonomous robot with wheels, it is assumed that the victims or obstacles lie of the ground. Hence the choice of the polar angle range is conducive. For better training and estimation performance, the range of the azimuth angle $\phi \in [-15°, 15°]$. The sensor can be mounted on a rotating platform so that the 30-degree range scans the 360-degree azimuth of the Cartesian coordinates. The polar range and azimuthal range are divided into 31 points each, i.e. a 1-degree step. This gives rise to a 31^2 number of data points. The data set is divided into training set (85%) and testing set (15%). The network is trained using the MATLAB's neural network toolbox with the parameters given in Table 1.

Table 1: Training Parameters.

Parameters	Values
Maximum number of Epochs	1000
Learning rate, μ	0.005
Learning rate decrement	0.01
Learning rate increment	10
Maximum learning rate	1×10^{10}
Minimum gradient	1×10^{-7}

4.1. On the number of hidden nodes

After series of simulations in which all other parameters were kept the same while varying the number of hidden layers, the best choice for H was found to be 30 number of hidden nodes as shown in Figure 1. Also, in some cases the network is tested with data that are not included in the training set; and data whose signal-to-noise ratio differs for that of the original training set.

4.2. Testing the trained network with unfamiliar data

The performance of the trained network is ascertained by generating a data set using direction-of-arrivals not included in the training set, at various signal-to-noise ratio. The root-mean-square error (RMSE) of the estimation versus the signal-to-noise ratio (SNR) is shown in Figure 2 for network trained with received with signal-to-noise of 15 dB.

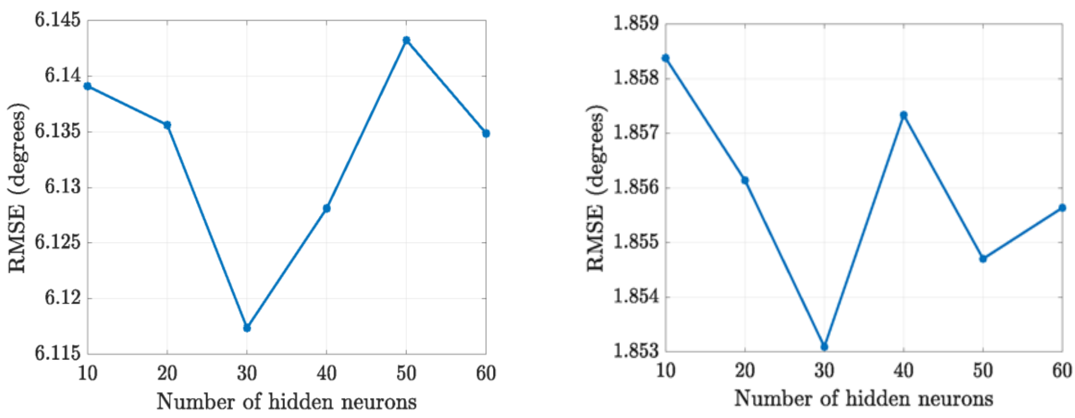

(a) (b)

Figure 1: Plot of RMSE versus the number of hidden nodes for signal-to-noise ratio of (a) 0dB and (b) 10dB.

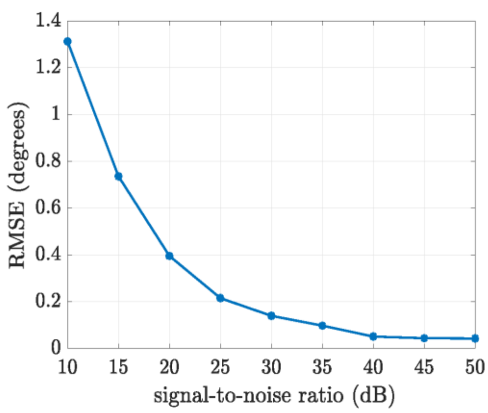

Figure 2: Root-mean-square error performance against various signal-to-noise-ratio.

Figure 2 shows that the higher SNR, the better the estimation performance of the trained network. Conversely, when tested with received data of lower SNR (i.e. 10 dB) the performance reduces by about 70%.

Conclusion

This paper developed a single-hidden layer Bayesian regularized multilayer perceptron artificial neural network for acoustic direction-of-arrival estimation. The signal processing adopted ensures the number of input nodes is less than what is obtainable in the open literature and the system is robust to additive noise in the received data. This system can be implemented in autonomous search-and-rescue robots in disaster areas for tracking victims by voice and avoiding obstacles. Further study can attempt widening the angular range of the system while achieving similar performance.

References

[1] NPR and Edison Research "The Smart Audio Report, Fall/Winter 2017", National Public Media, Washington D.C., USA, January, 2018. Accessed on: Dec. 19, 2018. [Online]. Available: https://www.nationalpublicmedia.com/smart-audio-report/previous-reports/

[2] A. Pikrakis, T. Giannakopoulos and S. Theodoridis, "Gunshot detection in audio streams from movies by means of dynamic programming and Bayesian networks," *2008 IEEE International Conference on Acoustics, Speech and Signal Processing*, Las Vegas, NV, 2008, pp. 21-24.

[3] Tokyo Institute of Technology, "'Listening' drone helps find victims needing rescue in disasters" (22-Dec-2017). [Online]. Available:https://www.titech.ac.jp/english/news/2017/040159.html, [Accessed on: 19-Oct-2018].

[4] J. Huang, "Sound Localization for Robot Navigation", in Robot Localization and Map Building, Chapter 25 [Online]. Rijeka:IntechOpen, 2010. Availble: https: // www. intechopen.com/ books/ robot- localization- and- map- building/ sound- localization- for-robot-navigation. [Accessed: 18-Oct-2018].

[5] J. Huang, T. Supaongprapa, I. Terakura, F. Wang, N. Ohnishi and N.Sugie, "A model-based sound localization system and its application to robot navigation", *Robotics and Autonomous Systems*, vol. 27, no. 4, June 1999, pp. 199-209.

[6] A. Nehorai & E. Paldi, "Acoustic vector-sensor array processing," *IEEE Transactions on Signal Processing*, vol. 42, no. 9, pp. 2481-2491, September 1994.

[7] MicroFlown, "Standard probes". [Online]. http://www.microflown.com/products/standard-probes/, [Accessed on: 19-Oct-2018].

[8] Y. I. Wu, K. T. Wong & S.-K. Lau, "The acoustic vector-sensor's nearfield array-manifold," *IEEE Transactions on Signal Processing*, vol. 58, no. 7, pp. 3946-3951, July 2010.

[9] Y. I. Wu, S.-K. Lau and K. T. Wong, "Near-field/far-field array manifold of an acoustic vector-sensor near a reflecting boundary," *Journal of the Acoustical Society of America*, vol. 139, no. 6, pp. 3159-3176, June 2016.

[10] C. J. Nnonyelu, "Pointing bias in "spatial matched filter" beamforming at a tri-axial velocity-sensor due to non-perpendicular axes", *World Journal of Innovative Research*, vol. 5, no. 2, pp. 24-29, August 2018.

[11] Y. Song and K. T. Wong, "Three dimensional localization of a nearfield emitter of unknown spectrum using an acoustic vector sensor," *IEEE Transactions on Aerospace and Electronic Systems*, vol. 49, no. 2, pp. 1035-1041, April 2013.

[12] D. Goryn and M. Kaveh, "Neural networks for narrowband and wideband direction finding," in the *Proceedings of ICASSP-88., International Conference on Acoustics, Speech, and Signal Processing*, vol. 4, New York, NY, USA, 1988, pp. 2164-2167.

[13] G. Arslan & F. A. Sakarya, "A unified neural-network-based speaker localization technique," *IEEE Transaction on Neural Networks*, vol. 11, no. 4, July 2000.

[14] G. Arslan, F. Gurgen & F. A. Sakarya, "Application of neural networks to bearing estimation," *Proc. Third IEEE International Conference on Electronics, Circuits, and Systems, ICECS '96*, vol.2, pp. 647-650.

[15] K. A. Gotsis, K. Siakavara & J. N. Sahalos, "On the direction of arrival (doa) estimation for a switched-beam antenna system using neural networks," *IEEE Transactions on Antennas & Propagation*, vol. 57, no. 5, pp. 1399-1411, May 2009.

[16] K. Gotsis, T. Kaifas, K. Siakavara & J. Sahalos, "Direction of arrival (doa) estimation for a switched-beam ds-cdma system using neural networks," *Proc. 19th International Conference on Applied Electromagnetics and Communications, ICECom*, 2007, pp. 1-4.

[17] K. A. Gotsis, E. G. Vaitsopoulos, K. Siakavara & J. N. Sahalos, "Multiple signal direction of arrival (doa) estimation for a switchedbeam system using neural networks," *PIERS Online*, vol. 3, no. 8, pp. 1160-1164, 2007.

[18] K. A. Gotsis, T. N. Kaifas, K. Siakavara & J. N. Sahalos "Direction of arrival (doa) estimation for a switched-beam DS-CDMA system using neural networks," *J. Automatika*, vol. 49, no. 1–2, pp. 27–33, 2008.

[19] Z. Stankovi, N. Donov, B. Milovanovi, J. Russer & I. Milovanovi, “Neural network approach for efficient ’doa’ determination of multiple stochastic em sources in far-field,” *International Conference on Numerical Electromagnetic Modeling and Optimization for RF, Microwave, & Terahertz Applications (NEMO)*, 2014, pp. 1-4.

[20] Z. Stankovic, et.al, “Localization of stochastic electromagnetic sources by using correlation matrix trained MLP neural network,” *Mikrotalasna Revija*, vol. 19, no. 2, pp. 44-49, 2013.

[21] D. Torrieri & K. Bakhru, “Simplification of the MUSIC algorithm using a neural network,” *Proc. Military Communications Conference, MILCOM*, 1996, vol. 3, pp. 873-876.

[22] N. Fonseca, M. Coudyser, J. Laurin & J. Brault, “On the design of a compact neural network-based DOA estimation system,” *IEEE Transactions on Antennas & Propagation*, vol. 58, no. 2, pp. 357-366, February 2010.

[23] M. Agatonovic, Z. Stankovic, N. Doncov, L. Sit, B. Milovanovic & T. Zwick, “Application of artificial neural networks for efficient highresolution 2D DOA estimation,” *Radioengineering*, vol. 21, no. 4, December 2012.

[24] A. H. El Zooghby, C. G. Christodoulou & M Georgiopoulos, “A neural network-based smart antenna for multiple source tracking,” *IEEE Transactions on Antennas & Propagation*, vol. 48, no. 5, pp. 768-776, May 2000.

[25] M. Wanga, S. Yangb, S. Wua & Feng Luoa, “A RBFNN approach for DoA estimation of ultra wideband antenna array,” *Neurocomputing*, vol. 71, no. 4, pp. 631–640, January 2008.

[26] A.H. EL Zooghby, H.L Southall & C. G. Christodoulou, “Experimental Validation of a Neural Network Direction Finder,” *IEEE Antennas and Propagation Society International Symposium*, 1999, vol.3, pp.1592-1595, July 1999.

[27] S. H. Zainud-Deen, H. A. Malhat, K. H. Awadalla & E. S. El-Hadad, “Direction of arrival and state of polarization estimation using radial basis function neural network (RBFNN),” *Progress In Electromagnetics Research B*, vol. 2, pp. 137–150, 2008.

[28] S. Vigneshwaran, N. Sundararajan & P. Saratchandran, “Direction of arrival (DoA) estimation under array sensor failures using a minimal resource allocation neural network,” *IEEE Transactions on Antennas and Propagation*, vol. 55, no. 2, pp. 334-343, February 2007.

[29] R. J. Mailloux & H. L. Southall “The analogy between the butler matrix and the neural-network direction-finding array,” *IEEE Antennas and Propagation Magazine*, vol. 39, no. 6, pp. 27-32, December 1997.

[30] T. K. Y. Lo, H. Leung & J. Litva, “Artificial neural network for AoA estimation in a multipath environment over the sea,” *IEEE Journal of Oceanic Engineering*, vol. 19, no. 4, pp. 555-562, October 1994.

[31] T. Lo, H. Leung & J. Litva, “Radial basis function neural network for direction-of-arrivals estimation,” *IEEE Signal Processing Letters*, vol. 1, no. 2, pp. 45-47, February 1994.

[32] Y. Kuwahara & T. Matsumoto, “Experiments on direction finder using RBF neural network with post-processing,” *Electronics Letters*, vol. 41, no. 10, May 2005.

[33] A. H. El Zooghby, C. G. Christodoulou & M. Georgiopoulos, “Performance of radial-basis function networks for direction of arrival estimation with antenna arrays, *IEEE Transactions on Antennas and Propagation*, vol. 45, no. 11, pp. 1611-1617, November 1997.

[34] H. L. Southall, J. A. Simmers & T. H. O’Donnell, “Direction finding in phased arrays with a neural network beamformer,” *IEEE Transactions on Antennas and Propagation*, vol. 43, no. 12, pp. 1369-1374, December 1995.

[35] R. L. Haupt, H. L. Southall & T. H. O’Donnell, “Biological beamforming,” in *Frontiers in Electromagnetics*, New York, IEEE Press, 2000, pp.329-370.

[36] E. Mochida & Y. Iiguni, “Adaptive doa estimation using a radial basis function network,” *Electronics and Communications in Japan*, part 3, Vol. 88, No. 9, 2005.

[37] T. O’Donnell, Jeff. Simmers, H. Southall & T. Klemas, “Neural beamforming for signal detection and location,” *Conference Record Military Communications Conference, MILCOM*, 1994, vol.2, pp. 326-330, October 1994.

[38] T. Wong, T. Lo, H. Leung, J. Litva & E. Bosse, “Low-angle radar tracking using radial basis function neural network,” *IEE Proceedings-F*, vol. 140, no. 5, pp. 323-328, October 1993.

[39] M. Agatonovic, Z. Stankovic, B. Milovanovic, & N. Doncov, “DOA estimation using radial basis function neural networks as uniform circular antenna array signal processor,” *10th International Conference on Telecommunication in Modern Satellite Cable and Broadcasting Services (TELSIKS)*, 2011, vol.2, pp.544-547, October 2011.

[40] M. Agatonovic & Z. Stankovic, “Hybrid ann model for accurate 2d doa estimation of a radiating source,” *11th International Conference on Telecommunication in Modern Satellite Cable and Broadcasting Services (TELSIKS)*, 2013, vol. 2, pp. 370-373, October 2013.

[41] H. Bertrand, D. Grenier & S. Roy, “Experimental antenna array calibration with artificial neural networks,” *Signal Processing*, vol. 88, no. 5, pp. 1152–1164, May 2008.

[42] H. Tang, T. Qiu, S. Li, Y. Guo & W. Zhang, "Robust Direction of Arrival (DOA) Estimation Using RBF Neural Network in Impulsive Noise Environment," in *Advances in Neural Networks*, Berlin Heidelberg, Germany, Springer , 2005, pp. 332-337.

[43] Y. Song, Y. L. Li and K. T. Wong, "Acoustic direction finding using a pressure sensor and a uniaxial particle velocity sensor," *IEEE Transactions on Aerospace and Electronic Systems*, vol. 51, no. 4, pp. 2560-2569, October 2015.

[44] MathWorks® MATLAB® documentation, 'Feedforwardnet'.[Online]. Available: https:// www.mathworks.com/ help/ deeplearning/ ref/ feedforwardnet. html, [Accessed on: 20-Oct-2018].

[45] R. Rojas, Neural Networks, Berlin, Germany, Springer-Verlag, 1996.

[46] D. J. C MacKay, "Bayesian Interpolation", *Neural Computation*, vol. 4, no. 3, pp. 415-447, 1992.

[47] F. Dan Foresee and M. T. Hagan, "Gauss-Newton approximation to Bayesian learning," *Proceedings of International Conference on Neural Networks (ICNN'97)*, vol.3., Houston, TX, USA, 1997, pp. 1930-1935.